SPACE-TIME EIGENRAKE AND DOWNLINK EIGENBEAMFORMER: EXPLOITING LONG-TERM AND SHORT-TERM CHANNEL PROPERTIES IN WCDMA

Christopher Brunner,[1,3] Joachim S. Hammerschmidt,[2] Alexander Seeger,[3] and Josef A. Nossek [1]

1. Institute for Circuit Theory and Signal Processing
Munich Univ. of Technology,
D-80290 Munich, Germany

2. Institute for Integrated Circuits,
BRIDGELAB Communications
Munich Univ. of Technology,
D-80290 Munich, Germany

3. Siemens AG
Hofmannstr. 51
D-81359 Munich
Germany

E-Mail: C.Brunner@ei.tum.de, J.Hammerschmidt@ei.tum.de, Nossek@ei.tum.de

Abstract - **For WCDMA base stations using adaptive antennas, we present a new space-time rake structure for uplink reception. Our approach combines short-term and long-term spatial and temporal channel properties using an eigenanalysis. By choosing dominant eigenbeams in time and space, the algorithm enhances interference suppression as well as spatial and temporal receive diversity. In contrast to previously introduced well-known receiver structures, the space-time eigenrake inherently adapts to different propagation environments and achieves higher spectral efficiency than other receivers, e.g., the beamformer rake. This is illustrated by Monte-Carlo simulations. Finally, we extend the proposed concept to the downlink, improving closed-loop downlink diversity compared to other proposals in standardization. Even though the feedback rate remains unchanged, additional antenna elements can be included to increase antenna and diversity gains.**

1. INTRODUCTION

The performance of digital mobile radio communication systems is limited by fast fading and interference from co-channel users. Both effects can be reduced by the use of antenna arrays at the base station with the appropriate signal processing, i.e., by diversity combining [9] and multiuser interference suppression. Several well-known rake receiver structures can be applied to DS-CDMA systems like WCDMA with adaptive antennas at the BS. These are, for instance, the maximum-ratio-combining rake in space and time [5], the decoupled space-time rake [5, 7], the joint space-time rake [5, 7], and the beamformer rake [11, 7]. The first three rake receivers differ only in interference suppression. The maximum-ratio-combining rake in space and time does not take interference into account and is optimal only for white noise in space and time. The decoupled space-time rake suppresses interference in space, whereas the joint space-time rake suppresses interference in space and time and, therefore, has the highest degrees of freedom. As these receivers structures use only short-term channel information they suffer from inaccurate channel estimation.

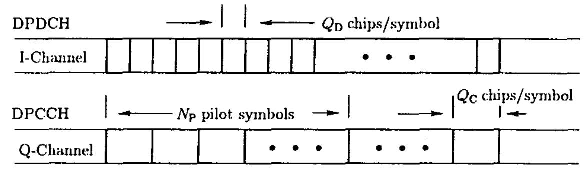

Figure 1: Uplink slot structure of WCDMA: A combination of code and IQ multiplexing is used. Moreover, N_P pilot symbols are transmitted at the beginning of each DPCCH slot.

The beamformer rake averages over a longer time period to obtain improved channel estimates, setting up long-term optimal spatial weights per (temporal) rake finger. It is well-suited for spatially correlated environments, providing interference suppression in the spatial domain. However, due to a lack of adaptivity to short-term channel variations, spatial diversity is lost.

After discussing signal model and channel model in Section 2, the new space-time eigenrake receiver is proposed in Section 3. In Section 4, simulation results are discussed. Finally, Section 5 applies the idea of the space-time eigenrake to the downlink and Section 6 draws the conclusions.

2. DATA MODEL

2.1. WCDMA Uplink Signal Model

WCDMA has two types of dedicated physical channels, the dedicated physical control channel (DPCCH) and the dedicated physical data channel (DPDCH), cf. Figure 1. On the uplink, the DPDCH baseband signal of the user of interest is expressed as

$$s_D(t) = \sum_{\ell=-\infty}^{\infty} b_D^{(\ell)}\, z_D(t-\ell T_D), \quad z_D(t) = \sum_{j=1}^{Q_D} d_D^{(j)}\, p(t-jT_c).$$

The chip rate is denoted by $1/T_c$. Moreover, the spreading sequence of the DPDCH, $z_D(t)$, is of length $T_D = Q_D T_c$ and is composed of Q_D chips $d_D^{(j)} \in \{-1, 1\}$, $1 \leq j \leq$

Q_D. The symbols, $b_D^{(\ell)} \in \{-1, 1\}$, are BPSK modulated. WCDMA uses a chip waveform, $p(t) \in \mathbb{R}$, characterized by a square-root raised cosine spectrum with a rolloff factor of $\alpha = 0.22$. In the same way, the DPCCH baseband signal of the user of interest is given by

$$s_C(t) = \sum_{\ell=-\infty}^{\infty} b_C^{(\ell)}\, z_C(t-\ell T_C), \quad z_C(t) = \sum_{j=1}^{Q_C} d_C^{(j)}\, p(t-jT_c),$$

where the spreading sequence of the DPCCH, $z_C(t)$, is of length $T_C = Q_C T_c$. Note that DPDCH and DPCCH may use different spreading codes. Then they are mapped to the I and Q branches according to [1]

$$s(t) = \beta \cdot s_D(t) + \mathrm{j} \cdot s_C(t), \qquad (1)$$

where β denotes the magnitude of the DPDCH in relation to the DPCCH. For simplicity, we do not include scrambling in our notation.

2.2. Channel Model

We assume that the narrowband assumption holds. Hence, each wave arriving at different antenna elements can be characterized by phase shifts. The baseband representation of the $M \times 1$ array snapshot vector $\boldsymbol{x}(t)$ containing the outputs of each of the M antenna elements after the channel filter at time t is modeled as

$$\begin{aligned} \boldsymbol{x}(t) &= \sum_{l=1}^{L^{(1)}} \xi_l^{(1)} \boldsymbol{a}^{(1)}(\mu_l) s^{(1)}(t-\tau_l^{(1)}) * p(t) \qquad (2) \\ &+ \sum_{k=2}^{K} \sum_{l=1}^{L^{(k)}} \xi_l^{(k)} \boldsymbol{a}^{(k)}(\mu_l) s^{(k)}(t-\tau_l^{(k)}) * p(t) + \boldsymbol{n}(t), \end{aligned}$$

where $\boldsymbol{a}^{(k)}(\mu_l)$, $\tau_l^{(k)}$, and $\xi_l^{(k)}$ denote the steering vector, the delay, and the time-variant complex amplitude of the l-th wavefront of the k-th user, respectively. The number of impinging wavefronts of the kth user is given by $L^{(k)}$, and the convolution operator is denoted by $*$. Moreover, the maximum channel delay spread in samples is denoted by $N_d = M_c \frac{\tau_{\max}}{T_c}$, where M_c is the oversampling factor and $\tau_{\max}$ is the maximum delay spread. In the sequel, we assume that the different receivers are synchronized to the beginning of a slot and that user 1 is the user of interest.

3. SPACE-TIME EIGENRAKE

To motivate the new receiver concept, characteristics of the beamformer rake and the conventional time-only rake are briefly discussed.

The beamformer rake [11, 7] exploits the long-term channel properties[1] by estimating the long-term spatial signal covariance matrix $\boldsymbol{R}_S^{(S)}(n)$ for each of the $1 \le n \le N_f$ rake fingers. With the corresponding interference covariance matrix $\boldsymbol{R}_{IN}^{(S)}(n)$, the spatial filter $\boldsymbol{w}^{(n)}$ which is the largest generalized eigenvector of the matrix pencil

$$\max_{\boldsymbol{w}(n)} \frac{\boldsymbol{w}^H(n)\boldsymbol{R}_S^{(S)}(n)\boldsymbol{w}(n)}{\boldsymbol{w}^H(n)\boldsymbol{R}_{IN}^{(S)}(n)\boldsymbol{w}(n)} \qquad (3)$$

is calculated. Since short-term channel estimation takes place after the spatial filters corresponding to the (temporal) rake fingers, channel estimation is improved by the antenna gain of the spatial filter. Moreover, the computational complexity required for channel estimation and subsequent processing is reduced considerably. This scheme performs well for spatially correlated channels. However, in case of channels which are spatially uncorrelated, both $\boldsymbol{R}_S^{(S)}(n)$ and $\boldsymbol{R}_{IN}^{(S)}(n)$ have diagonal structure, and, consequently, one of the entries of $\boldsymbol{w}(n)$ is large and all others are small. In this case, antenna gain/interference suppression degrades.

Let us now briefly review the conventional (time-domain) rake receiver [12]. The complete short-term channel estimate in time $\boldsymbol{h}^{(T)}(i) \in \mathbb{C}^{N_d}$ (of one antenna) can be obtained by correlation with the pilot sequence which is part of the above defined control channel $s_C(t)$, where i and N_d denote the slot number and the maximum delay spread in samples, respectively. If $\boldsymbol{h}^{(T)}(i)$ is wide-sense-stationary (WSS) [4], the long-term temporal signal covariance matrix equals[2]

$$\boldsymbol{R}_S^{(T)} = \mathrm{E}\{\boldsymbol{h}^{(T)}(i)(\boldsymbol{h}^{(T)}(i))^H\}. \qquad (4)$$

Since uncorrelated scattering (US) [4] is assumed, $\boldsymbol{R}_S^{(T)}$ is diagonal and the contributions of temporal taps selected for further processing steps are uncorrelated. Hence, temporal diversity is fully exploited[3].

In contrast, the spatial channel estimates $\boldsymbol{h}^{(S)}(i)$ (for one temporal tap) are correlated for most scenarios. The entries of the long-term spatial correlation matrix,

$$\boldsymbol{R}_S^{(S)} = \mathrm{E}\{\boldsymbol{h}^{(S)}(i)(\boldsymbol{h}^{(S)}(i))^H\} \qquad (5)$$

depend on the spatial distribution of wave incidence power for the given temporal tap. Clearly, in contrast to dropping temporal taps, it is not recommendable to drop the output of some of the antenna elements to increase performance and reduce complexity. However, a similar approach can

[1] The time-variant mobile radio channel is subject to short-term and long-term fluctuations. The short-term fluctuations are caused by Doppler shifts, i.e., by the velocity of the mobile. The long-term fluctuations are due to different positions of the mobile.

[2] If the WSS assumption holds, the second order statistics of the signals remain constant over time, i.e., the long-term channel properties stay constant. This, of course, is not the case in real systems, where a forgetting factor should be applied when averaging.

[3] More precisely, adjacent taps are typically correlated due to oversampling by $M_c = 2$. Therefore, adjacent taps are not selected by the rake searcher.

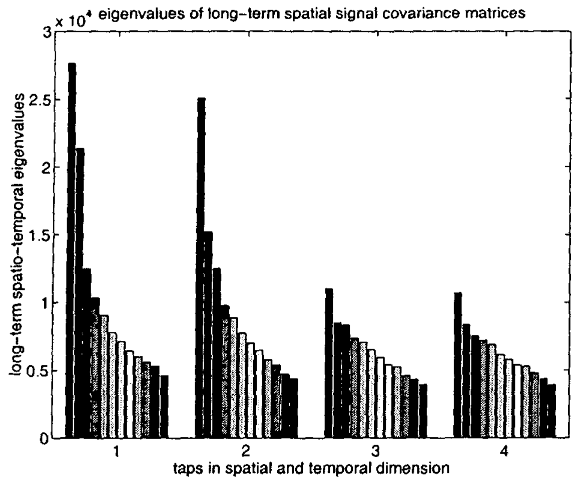

Figure 2: Long-term spatial eigenvalues of four temporal taps for a spatially selective scenario.

be applied after performing a transformation of spatial measurements. In order to find a suitable transformation, let us state two major goals:

- The transformed outputs should be as uncorrelated as possible to maximize the diversity gain using a small number of spatial filters.
- The spread of the mean (long-term) signal to interference and noise ratio (SINR) of the transformed outputs should be maximized to maximize the interference suppression for a small number of spatial filters.

These goals are jointly optimized by carrying out a generalized eigenvalue decomposition of the long-term spatial covariance matrices[4],

$$\boldsymbol{\Theta} = \boldsymbol{W}^{-1}\, \boldsymbol{R}_{\mathrm{IN}}^{-1}\, \boldsymbol{R}_{\mathrm{S}}^{(\mathrm{S})}\, \boldsymbol{W}, \tag{6}$$

where

$$\boldsymbol{W} = \begin{bmatrix} \boldsymbol{w}_1^{(\mathrm{S})} & \boldsymbol{w}_2^{(\mathrm{S})} & \dots & \boldsymbol{w}_M^{(\mathrm{S})} \end{bmatrix}$$

denotes the eigenvectors and the diagonal matrix $\boldsymbol{\Theta}$ contains the corresponding eigenvalues. The *spatial rake searcher* selects the eigenvectors belonging to the dominant eigenvalues which serve as spatial filters. Thus, similarly to selecting dominant temporal taps whilst neglecting others, the spatial dimension is reduced from the number of antenna elements to the number of selected eigenvalues.

The spatial eigenrake can easily be extended to frequency selective channels. The structure of the resulting space-time eigenrake is depicted in Fig. 3. In Fig. 2, the long-term spatial eigenvalues of four temporal taps are plotted for a spatially selective scenario. Accordingly, the four largest eigenvalues belong to the first two temporal taps. Therefore, if four rake fingers are allowed, in the present scenario these would be applied to the first two taps only by using the two corresponding eigenvectors for each tap as spatial filters. (In contrast, the beamformer rake would deploy one rake finger per temporal stage and use the dominant eigenvector of this temporal stage only.) By taking into account the long-term spatio-temporal structure of the mobile radio channel, *short-term processing* is improved with respect to computational complexity and accuracy of the (compressed) spatio-temporal channel estimate[5]. In notational terms, the overall procedure can be put in the following form. We construct a spatial compression matrix from the spatial filters selected by the space-time rake searcher according to

$$\boldsymbol{C}^{(\mathrm{S})} = \begin{bmatrix} \boldsymbol{w}_1 & \boldsymbol{w}_2 & \cdots & \boldsymbol{w}_{N_{\mathrm{f}}} \end{bmatrix} \in \mathbb{C}^{M \times N_{\mathrm{f}}}. \tag{7}$$

Likewise, we can construct a temporal compression matrix $\boldsymbol{C}^{(\mathrm{T})} \in \mathbb{R}^{N_{\mathrm{d}} \times N_{\mathrm{f}}}$. All entries of n-th column of $\boldsymbol{C}^{(\mathrm{T})}$ are "0"s, except for a single "1" at the position of the n-th temporal rake finger. This position is associated with a spatial filter and is determined by the space-time rake searcher. Then the compressed space-time vectors *before* and *after* the correlator are defined as

$$\boldsymbol{x}_{\mathrm{c}}^{(l)} = \mathrm{diag}\left\{ \boldsymbol{C}^{(\mathrm{S})H} \mathcal{X} \boldsymbol{J}^{(l)} \boldsymbol{C}^{(\mathrm{T})} \right\}, \tag{8}$$

$$\boldsymbol{h}_{\mathrm{c}} = \mathrm{diag}\left\{ \boldsymbol{C}^{(\mathrm{S})H} \mathcal{H} \boldsymbol{J}^{(1)} \boldsymbol{C}^{(\mathrm{T})} \right\}, \tag{9}$$

where the rows of the data matrices $\mathcal{X} \in \mathbb{C}^{M \times N}$ and $\mathcal{H} \in \mathbb{C}^{M \times N}$ contain the spatial snapshots $\boldsymbol{x}(t)$ and $\boldsymbol{h}(t)$ sampled at M_c times the chip rate $1/T_c$ *before* and *after* the (pilot) correlator, respectively. Moreover, a temporal selection matrix

$$\boldsymbol{J}^{(l)} = \begin{bmatrix} \boldsymbol{0}_{(l-1) \times N_{\mathrm{d}}} \\ \boldsymbol{I}_{N_{\mathrm{d}} \times N_{\mathrm{d}}} \\ \boldsymbol{0}_{(N-l-N_{\mathrm{d}}+1) \times N_{\mathrm{d}}} \end{bmatrix}$$

is applied to the correlator output $\mathcal{H}$ such that $\mathcal{H}\boldsymbol{J}^{(1)} \in \mathbb{C}^{M \times N_{\mathrm{d}}}$ contains all multipath components. The short-term compressed measurement covariance matrix equals

$$\boldsymbol{K}_{\mathrm{X}}^{(\mathrm{C})} = \mathrm{mean}\left\{ \boldsymbol{x}_{\mathrm{c}}^{(l)} \cdot \boldsymbol{x}_{\mathrm{c}}^{(l)H} \right\}. \tag{10}$$

Note that l is limited to the spatial snapshots within the time coherence of the channel. Assuming that the channel stays approximately constant for at least one slot, the compressed space-time weight vector $\boldsymbol{w}_{\mathrm{c}}$ can be found by solving $\boldsymbol{h}_{\mathrm{c}} = \boldsymbol{K}_{\mathrm{X}}^{(\mathrm{C})} \boldsymbol{w}_{\mathrm{c}}$. Short-term interference suppression supports long-term interference suppression especially if, for instance, the channel is spatially uncorrelated.

[4]Note that $\boldsymbol{R}_{\mathrm{IN}}$ is estimated by averaging over the outer product of the spatial snapshots given by $\boldsymbol{x}(t)$, cf. (2). Since the signal of interest is significantly weaker than the sum of interfering signals in WCDMA, it is not necessary to extract the signal part.

[5]Note that in contrast to previously known dimension reduction techniques [2], the eigenbeam concept exploits the long-term channel properties in an optimal fashion [10] compared to, e.g., using a fixed Butler matrix.

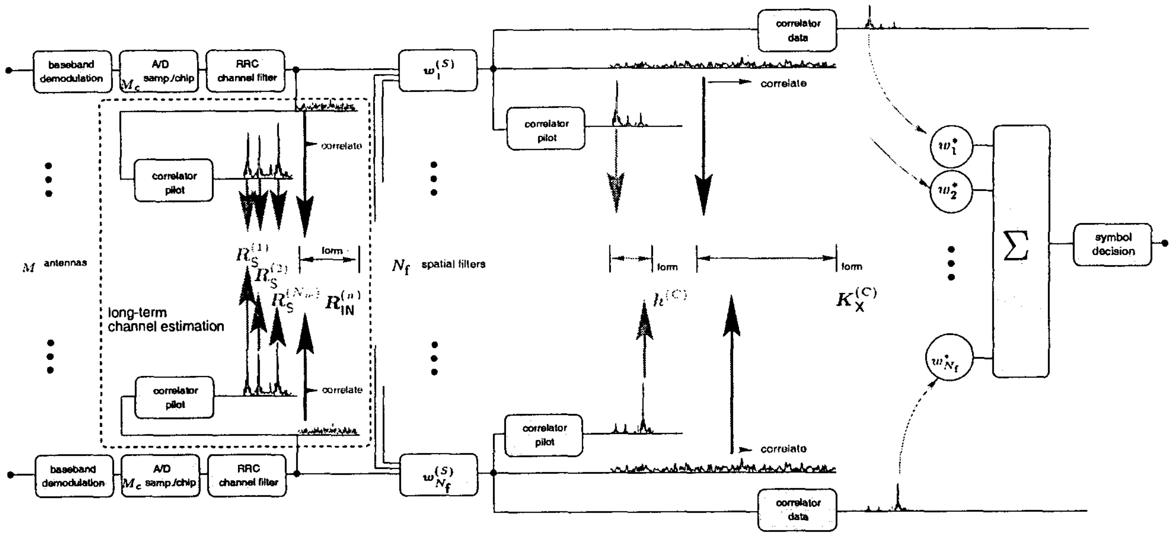

Figure 3: Structure of the space-time eigenrake.

4. SIMULATIONS

The simulation results are based on a rural and a pico environment [6], cf. Fig. 4. The rural environment is characterized by a maximum delay spread of $N_{\mathrm{d}} = 7$ samples and a large Doppler spread ($v_{\mathrm{mob}} = 100$km/h). As the distance between BS and mobile is large and scatterers are close to the mobile, the channel is spatially correlated. Interference is modelled by a service mix with 5 times as many weak speech users ($Q_{\mathrm{D}} = 128$) as strong high-data-rate users ($Q_{\mathrm{D}} = 8$). The pico environment has a delay spread of $N_{\mathrm{d}} = 11$ samples and a smaller Doppler spread ($v_{\mathrm{mob}} = 50$km/h). As there are many scatterers near the BS, the spatial correlation of the channel is low. Hence, interference is modelled by white spatial and white temporal noise passed through the channel filter. The eigenvalue profile shown in Fig. 2 has been generated in this pico environment.

We focus on three different types of rake receivers, i.e., the decoupled space-time rake which exploits long-term channel information only to determine the temporal rake fingers, the beamformer rake which considers only the strongest generalized eigenvector of each (temporal) rake finger in the long term, and the space-time eigenrake which takes the long-term space-time channel information fully into account. Simulation parameters are as follows: uniform linear array with an antenna distance of 0.5λ; $M_c = 2$; user of interest: $\beta = 2$, $Q_{\mathrm{D}} = 128, N_{\mathrm{P}} = 6$ pilot symbols/slot; simulated time: 500 ms; channel estimate limited to one slot; perfect power control; $N_{\mathrm{f}} = 4$ rake fingers[6]. Our performance measure is the raw bit error ratio (BER)[7]. The performance gain in SIR achieved by the space-time eigenrake compared to the beamformer rake is approximately 2 dB in the pico environment, cf. Fig. 4 top right. In the rural environment, the space-time eigenrake and the beamformer rake perform similarly[8]. The slight superiority of the space-time eigenrake is explained by its short-term interference suppression. Moreover, the space-time eigenrake always performs better than the decoupled space-time rake although fewer correlations are required, cf. also [7].

5. DOWNLINK EIGENBEAMFORMER

With orthogonal pilots transmitted at each BS antenna element, the spatio-temporal downlink channel can be estimated at the mobile. However, the feedback rate is limited (to one bit per slot). The current version of the standard [1] contains a closed-loop TX diversity scheme where the mobile feeds back downlink beamforming commands describing relative phase shifts to be applied to the second of two transmit antennas [13]. A straightforward extension towards four antenna elements has been suggested. Since, however, e.g., quantization is rough and diversity is lost in spatially non-coherent time-variant scenarios, performance degrades. Here, the downlink eigenbeamformer provides a valuable remedy [8, 7]. The dominant (long-term) eigenbeams can be determined at the mobile and made available at the BS using an extremely low feedback rate. If the coherence time of the channel is large enough, the mobiles

[6]The decoupled space-time rake generates as many diversity branches as antenna elements times rake fingers, $M \cdot N_{\mathrm{f}}$, whereas beamformer and eigenrake limit the number of branches to the number of rake fingers N_{f}. Correlations for channel estimation and data detection are required for each branch.

[7]A raw BER smaller than 12 % is required to ensure a sufficient BER after decoding for uplink WCDMA.

[8]In spatially correlated scenarios, the space-time eigenfingers are the same for beamformer and eigenrake.

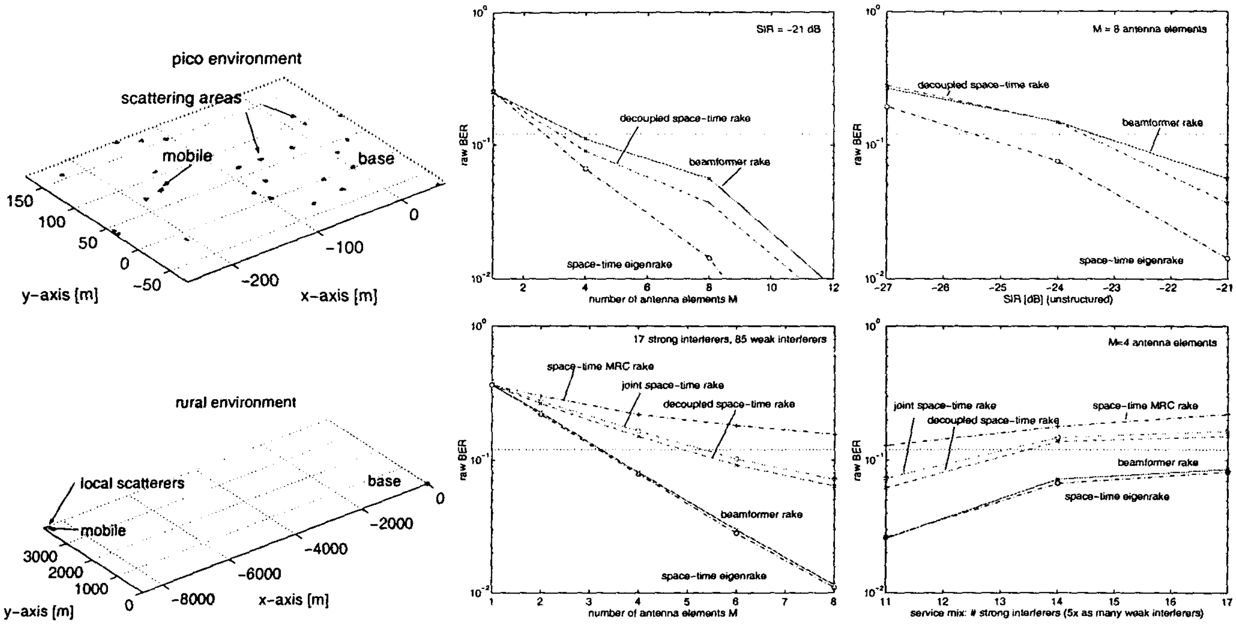

Figure 4: Upper row: pico environment, lower row: rural environment.

determine the stronger short-term eigenbeam out of a subset of, e.g., two dominant eigenbeams. The index to this eigenbeam is fed back to the BS using one bit/slot. The BS uses the selected eigenbeam for downlink transmission[9].

6. CONCLUSIONS

In the context of future WCDMA cellular communication systems, we have introduced a novel rake receiver structure, the *space-time eigenrake*. The concept is based on using an eigenanalysis for each temporal tap and performing a spatio-temporal rake search. By the latter, the overall dominant eigenvalues are selected and the corresponding eigenvectors are used as weight vectors within the respective temporal stage. Despite low complexity, the new structure outperforms previously known concepts such as the beamformer rake or the decoupled space-time rake. The eigenrake automatically adjusts to various propagation environments which is another major advantage, whereas known concepts are typically well-suited only for some scenarios but less so for others. Moreover, we have extended the general idea to the downlink. The downlink eigenbeamformer is currently discussed in WCDMA standardization bodies (3GPP). Improved diversity, antenna gain, and interference suppression can be achieved by increasing the number of elements while maintaining a feedback rate of one bit/slot.

[9]Alternatively, long-term channel estimates can be obtained from the uplink. Then the frequency gap must be considered, cf. [3], and calibration must take place.

7. REFERENCES

[1] *Third Generation Partnership Project (3GPP)*, 2000, http://www.3gpp.org.

[2] S. Anderson, *On Dimension Reduction in Sensor Array Signal Processing*, Ph. D. dissertation, Department of Electrical Engineering, Linköping University, Linköping, Sweden, 1992.

[3] T. Aste, P. Forster, and L. Fety, "Downlink beamforming avoiding DOA estimation for cellular mobile communications", in *Proc. IEEE Int. Conf. Acoust., Speech, Signal Processing*, Seattle (USA), 1998.

[4] P. A. Bello, "Characterization of randomly time-variant linear channels", *IEEE Transactions on Communication Systems*, vol. CS-11, pp. 360–393, Dec. 1963.

[5] X. Bernstein and A. M. Haimovich, "Space-time optimum combining for CDMA communications", *Wireless Personal Communications*, vol. 3, pp. 73–89, 1996, Kluwer Academic Publishers.

[6] J. J. Blanz and P. Jung, "A flexibly configurable spatial model for mobile radio systems", *IEEE Trans. Communications*, vol. 46, pp. 367–371, Mar. 1998.

[7] C. Brunner, *Efficient Space-Time Processing Schemes for WCDMA*, Ph. D. dissertation, Munich University of Technology, Institute for Circuit Theory and Signal Processing, Munich, Germany, June 2000.

[8] C. Brunner, J. S. Hammerschmidt, and J. A. Nossek, "Downlink Eigenbeamforming in WCDMA", in *European Wireless 2000*, Dresden, Germany, Sept. 2000.

[9] J. S. Hammerschmidt and C. Brunner, "The implications of array and multipath geometries in spatial processing", in *Proc. IEEE / IEE Int. Conf. on Telecommunications*, Acapulco, Mexico, May 2000.

[10] J. S. Hammerschmidt, C. Brunner, and C. Drewes, "Eigenbeamforming - a novel concept in array signal processing", in *European Wireless 2000*, Dresden, Germany, Sept. 2000.

[11] B.H. Khalaj, A. Paulraj, and T. Kailath, "2-D rake receivers for CDMA cellular systems", in *Proc. IEEE GLOBECOM*, pp. 400–404, 1994.

[12] J. G. Proakis, *Digital Communications*, McGraw-Hill, New York, NY, 3rd edition, 1995.

[13] M. Raitola, A. Hottinen, and R. Wichman, "Transmission diversity in wideband CDMA", in *Proc. 49th IEEE Vehicular Technology Conf. Spring (VTC '99 Spring)*, pp. 1545–1549, Houston, Texas, May 1999.